Ionization and Dissociation of Benzaldehyde Using Short Intense Laser Pulses

D. J. Smith, K. W. D. Ledingham,* H. S. Kilic,† T. McCanny, W. X. Peng, and R. P. Singhal

Department of Physics & Astronomy, University of Glasgow, Glasgow, G12 8QQ Scotland, UK

A. J. Langley and P. F. Taday

Central Laser Facility, Rutherford Appleton Laboratory, Didcot, Oxon, OX11 0QX England, UK

C. Kosmidis

Department of Physics, University of Ionannina, Greece

Received: November 14, 1997; In Final Form: January 31, 1998

In a recent series of experiments, femtosecond laser mass spectrometry (FLMS) was applied to benzaldehyde utilizing laser pulse widths in the range 90 fs to 2.7 ps. Beam intensities up to 2×10^{14} W cm^{-2} were used with wavelengths of 750 and 375 nm. Different ionization−dissociation channels were found compared with previous studies by other authors based in the nanosecond regime. The general theme emerging is one of predominant above-threshold ionization−dissociation (ID) in which predissociative states are largely bypassed via rapid optical up-pumping to the molecular ionization continuum. Above the parent ionization threshold, ladder-switching is seen to be a function of laser pulse width, intensity, and wavelength with exclusive parent ion formation being achievable in the lower intensity regions at all pulse widths. Increasing fragmentation occurs as the laser intensity increases, although parent supremacy remains. At 750 nm however, the increase of fragmentation with intensity is greatly reduced compared to 375 nm, leading to the conclusion that FLMS at longer wavelengths is preferred for chemical analysis. Moreover at 750 nm and at laser intensities close to 10^{14} W cm^{-2} $C_7H_6O^{2+}$ becomes evident. It is also shown that the $C_7H_6O^+/C_7H_5O^+$ ratio is strongly dependent on the pulse width, suggesting that a hydrogen loss pathway has a dissociation time of about a picosecond.

Introduction

Photoionization and photodissociation investigations of polyatomic molecules are of current theoretical and experimental interest. The advent of commercially available short-pulse-width lasers has fuelled this interest in terms of approaching saturation ionization efficiencies (100% ionization) coupled with clearer insights into molecular structure and ionization/dissociation pathways.

Multiphoton absorption in molecules can lead to fragmentation by two distinct mechanisms.[1−3]

(1) Dissociation−Ionization (DI). The molecule in an excited state below the ionization level fragments to form neutral moieties. These fragments may absorb further photons within the laser pulse to ionize and/or dissociate. If the intermediate excited states have lifetimes shorter than the laser pulse width, then dissociation followed by ionization (DI), ladder-switching, is favored.

(2) Ionization−Dissociation (ID). Efficient multiphoton absorption of photons can suppress fragmentation channels in the sense that rapid up-pumping to the molecular ion continuum can bypass predissociative states. This usually requires laser pulse widths shorter than intermediate state lifetimes. This is ionization followed by dissociation (ID), or ladder-climbing. Dissociation can then occur via a myriad of ionic states, depending on laser intensity, pulse width, and wavelength.

Molecular predissociation often competes with ladder climbing, the latter becoming more dominant as the laser pulse duration decreases.[1] Laser intensities may be used to control the degree of fragmentation, especially in the above-threshold (ID) model. This can allow exclusive molecular ion formation, which has significant implications for chemical analysis. In general, choice of laser intensity and pulse width reflects the goals of the experiment.

In a series of papers[2,4−8] the Glasgow group has shown that FLMS is becoming a universal system for the analytical detection of molecules, in which DI suppression and abundant parent ion appearance are consistently attained. This is coupled to reduced relative intensities of lighter mass fragments in the mass spectra. FLMS can also provide valuable information on ionization/dissociation pathways and the associated dissociative lifetimes.

The mechanism of ionization itself is being challenged in that nonperturbative physics may provide a more complete description than multiphoton theories.[9,10] In addition nonstatistical energy migration within the molecules upon photon absorption is probable, leading to selective local dissociation.[11] This may develop an increased understanding in energy flow and interaction within molecular systems. Thus the potential for FLMS in both theoretical and applied science is considerable.[2,4−15]

Benzaldehyde photoprocesses have generated considerable interest (ref 16 and references therein). The molecule's ionization potential is 9.52 eV.[17] Electronic excitation to the first singlet excited state (S_1) gives rise to a weak absorption band

† Permanent address: Department of Physics, University of Selcuk, 42079 Konya, Turkey.

* Author for correspondence. E-mail: k.ledingham@physics.gla.ac.uk.

S1089-5639(98)00212-6 CCC: $15.00
Published on Web 03/24/1998

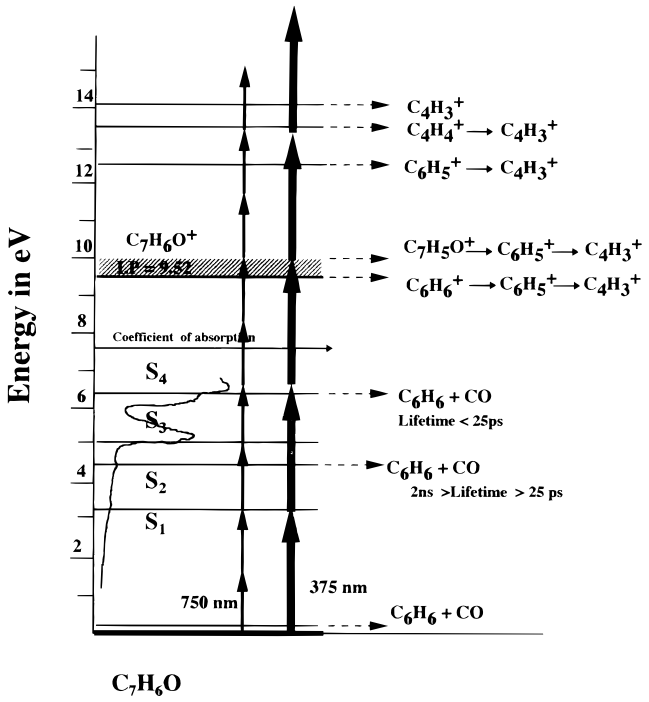

Figure 1. Some of the energetically allowed fragmentation pathways in the neutral and ionic manifold of states. The absorption spectrum for benzaldehyde is also shown as well as the absorption of nine photons at 750 nm and five photons at 375 nm.

system at 371.5 nm. The second absorption band to the S_2 state occurs at 4.51 eV (275 nm) while by far the strongest absorption peaks occur at 220−245 nm (∼5 eV, S_3) and at 194−195 nm (∼6.4 eV, S_4).[16−18] The triplet manifold is less well categorized, although intersystem crossing via T-states has been reported.[19,20] Figure 1 is a diagram showing some of the energetically allowed fragmentation pathways in the neutral and ionic manifold of states. The appearance potentials are taken from refs 1 and 18. The absorption spectrum for benzaldehyde is also shown as well as the absorption of nine photons at 750 nm and five photons at 375 nm.

The laser mass spectrometry of benzaldehyde has been investigated at varying laser pulse widths, intensities, and wavelengths. A primary process in benzaldehyde photolysis involves the formation of benzene and carbon monoxide (via the S_2 and S_4 states)[1,16−21] from below the molecular ionization threshold, thus suppressing molecular ion production. The products can then absorb further photons and ionize/fragment:

$$C_7H_6O + nh\nu \rightarrow C_7H_6O^* \rightarrow C_6H_6 + CO$$

Dissociation from the S_2 singlet occurs on a time scale less than 2 ns[17] but greater than 25 ps.[1] The S_4 singlet is thought to dissociate faster.[16]

A general theme emerging is as follows: nanosecond pulse lengths yield small or nonexistent parent ions, with a strong dominance of lighter mass fragments. This is consistent with below threshold dissociation−ionization (DI). DeCorpo et al.,[22] Seaver et al., [23] and Antonov et al.[21,24] show mass spectra for benzaldehyde at 20 ns with very low intensity parent or high mass peaks. Long et al.[17] report a similar conclusion, namely, that total dominance of lighter fragment ions occurs, indicating predissociation competing strongly with direct photoionization, specifically from the S_2 state. In this pulse length regime, the choice of wavelength is seen to significantly influence whether ladder-switching or -climbing occurs. Yang et al.[18] in a multiphoton investigation of benzaldehyde using laser pulse widths of 8 ns found competition between ID and DI pathways at 266 nm (one photon energy coincides with the S_2 band) which was also dependent on laser intensity. The molecule in the excited S_2 singlet would either dissociate or be effectively bypassed by optical pumping. However at 355 nm (one photon energy coincides with an S_1 state), irradiation at both nanosecond and picosecond times led to ID domination over the entire laser intensity range. They concluded that wavelength selection was a more important parameter in protecting the molecule against DI than laser intensity.

In the picosecond pulse width region, parentlike dominance over its moieties is largely found, in contrast to the nanosecond findings. A specific above-threshold dissociation pathway is

$$C_7H_6O + mh\nu \rightarrow C_7H_6O^+ \rightarrow C_7H_5O^+ + H$$

As with **nanosecond studies**, a wavelength influence on ionization dynamics is found. In another study Yang et al.[1] described the "immediate" dissociation of $C_7H_6O^+$ in the above pathway at 25 ps and 266 nm, whereas increasing the wavelength to 355 nm resulted in larger parent ion peaks. "Immediate" in this sense is presumed to mean less than 25 ps. They also suggested that the role of ladder-climbing increased as the laser pulse decreased from nanosecond to picosecond duration.

The present paper extends the previous measurements in the nanosecond and tens of picosecond regimes, describing recent experimental findings for benzaldehyde photochemistry. Time-of-flight (TOF) techniques are used with short, intense laser pulse durations ranging from 90 fs to 2.7 ps at wavelengths of 750 and 375 nm and using laser intensities up to 2×10^{14} W cm^{-2}. In particular it was of interest to investigate the fast hydrogen loss dissociative pathway and to determine at these short pulse widths and high laser intensities whether ID is the generally preferred dissociative mechanism similar to the results reported for other molecules carried out in this intensity regime.[2,7,8]

Experimental Section

Femtosecond Laser System. Technological advances in lasers are producing desirable results in terms of reliable short-pulse duration.[25] Figure 2 shows the femtosecond laser system coupled to the linear time-of-flight mass spectrometer used in this study. The time-of-flight[6] and laser[26] arrangements are described more extensively elsewhere. Pulses of 45 fs duration were derived from a mode-locked titanium-sapphire oscillator pumped with about 7 W from an all-lines Beamlok argon ion laser (both Spectra Physics). A simple stretcher consisting of two pairs of BK7 prisms in a double-pass arrangement was used to negatively chirp the pulses to about 700 fs prior to amplification in a three-stage dye laser. The dye LDS 751 was used in preference to the higher gain rhodamine 700, normally used at this wavelength, to provide sufficient gain bandwidth to support 45 fs pulses. After the amplifier a 4 cm block of SF10 glass allowed recompression of the pulses down to 50 fs, although they did lengthen to 90 fs prior to entry into the TOF after passage through the optical components shown in Figure 2.

The fundamental output harmonic, 750 nm, was collimated using a 1 m focal lens (f/50) to give a beam width of approximately 10 mm. A 0.5 m focal length fused silica lens focused the 750 nm light into a type I BBO crystal of width 200 μm cut at 28.7° to frequency double the beam. Additionally, a 750 nm half-wave plate was added before the 0.5 m focal

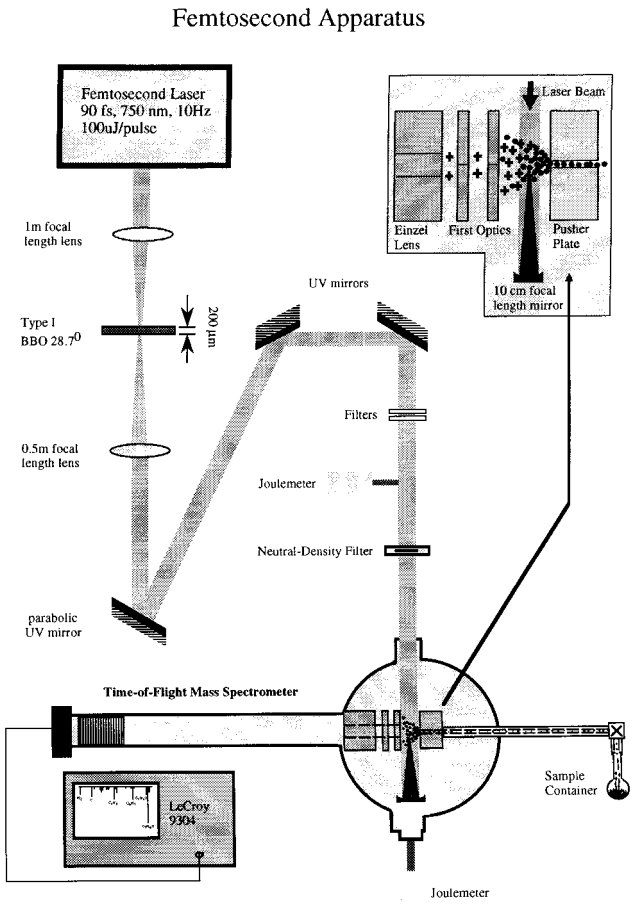

Figure 2. Experimental apparatus showing the femtosecond laser system coupled to the linear time-of-flight mass spectrometer. Pulse widths ranging from 90 fs to 2.7 ps were generated. Peak intensities were of the order of 2×10^{14} W cm^{-2} at wavelengths 750 and 375 nm.

length lens when frequency doubling. The 375 nm beam was therefore vertically polarized, consistent with the vertically polarized 750 nm output. The 750 and 375 nm light was recollimated with an off-axis 0.5 m focal length parabolic mirror with UV-enhanced aluminum. Further broad-band UV mirrors directed the laser pulses toward the mass spectrometer. For 375 nm, an infrared absorbing filter eliminated the presence of 750 nm light and background amplified stimulated emission (ASE). With 750 nm, energy measurements revealed an ASE content of about 25%. This was taken into account when determining the laser intensity. Controlled attenuation of the beam energy was achieved using a variable neutral density filter. The energies of the beam pulses were measured using a Molectron joulemeter.

Upon entering the TOF, the beam was focused using a concave mirror of focal length 10 cm, yielding calculated spot diameters of 5 and 10 μm for the 375 and 750 nm beams, respectively. As such, laser intensities from 7×10^{11} (375 nm) and 6×10^{12} (750 nm) up to 2×10^{14} W cm^{-2} for both wavelengths were generated. Laser intensities were estimated to be accurate to 10−15%.

Autocorrelation diagnostics[27] were used to measure the pulse widths for 750 nm and from these were inferred the pulse widths at 375 nm. Laser pulse durations from 90 fs to 1.32 ps (375 nm) and 2.7 ps (750 nm) were produced by lengthening the pulses after passage through various thickness of SF10 blocks. The laser energy and intensity fell sharply as the pulse width increased. Estimated errors in the autocorrelation measurements came from the nonuniformity of the beam intensity profile and pulse width broadening due to group velocity dispersion in the optical components of the correlator. Variation in pulse-to-pulse generation also contributed. As such an uncertainty in pulse length of ±10% was estimated.

Time-of-Flight Mass Spectrometer (TOF). The TOF is of conventional linear design, with a field-free drift region of 1.2 m. A turbo pump ensured a base pressure of 10^{-8} Torr, rising to approximately 10^{-5} Torr during active experimentation. Conditions were therefore essentially unimolecular since the collision probability was small. Ion optics was based on a Wiley−McLaren design and an einzel lens placed immediately after the extract optics increased the ion transmission through the system. The mass resolution was typically 200 at 100 D.

The benzaldehyde sample was admitted effusively from the inlet system to the high-vacuum environment via a needle valve, before passing through a tiny hole in the pusher electrode of the TOF. The position of the laser spot with respect to this opening was critical.[2] Optimum spatial ionizing conditions were achieved using an *xyz* vernier-controlled mechanism coupled to the focusing mirror to vary precisely the beam position. The inlet line to the TOF chamber was heated independently at 120 °C, which minimized the sample sticking to the walls. The entire TOF system could also be heated, which was very effective in creating a clean environment when coupled to efficient evacuation and occasional gas-flow flushing.

The time-of-flight mass spectra were recorded using a Thorn EMI electron multiplier coupled to the Lecroy 9304 digital oscilloscope, typically averaging over hundreds of laser shots.

Results and Discussion

Figure 3 shows the ionization−dissociation mass spectra at 750 and 375 nm for varying laser intensities up to 1.2×10^{14} W cm^{-2} at 90 fs pulse duration. It is clear that for both wavelengths at all intensities the parent peak is dominant. Fragmentation increases with increasing laser intensity and also becomes more prominent for the shorter wavelength. For analytical purposes, soft ionization with an exclusive parent ion formation is to be favored and is achieved for the lower laser intensities particularly for the longer wavelengths. This has important implications, particularly in multicomponent analysis, for example, environmental air monitoring.[28] On the other hand when structural information is sought, then significant molecular fragmentation is desirable which is obtained using higher laser intensities and shorter wavelengths. It is also important to point out that the doubly charged benzaldehyde ion is a strong peak under 750 nm irradiation and is not apparent in the 375 nm spectrum.

As a comparison, Figure 4 illustrates the mass spectra recorded by Yang et al.[1] at 355 nm and 25 ps. The parent peak again is predominant at all laser intensities suggesting an ID dissociative route as Yang et al. concluded. However, the dependence of the ion intensities as a function of laser power for the different fragments are markedly dissimilar, indicating that DI pathways are also open for some of the moieties. This point will be discussed in more detail later.

As previously stated, the fragmentation at 375 nm is considerably greater than at 750 nm. Thus the UV photons would seem less suitable for analytical purposes at these laser pulse widths, due to a lower production of intact molecular ions. Over the intensity range, the 375 nm daughter fragments show a factor of about 4 times greater intensity than at the longer wavelength.

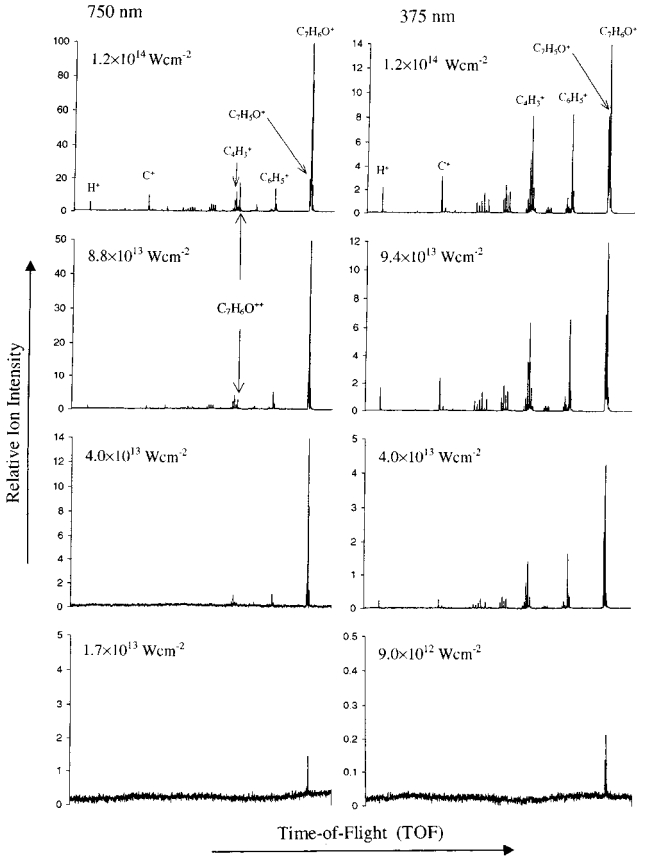

Figure 3. Ionization−dissociation mass spectra for benzaldehyde illustrating the relative ion yield against their corresponding time-of-flight for wavelengths 750 and 375 nm at 90 fs laser pulse widths. Laser intensities up to 1.2 × 10^{14} W cm^{-2} were used, and for any opposite pair of mass spectra intensities are as close as possible in value. The amplifier gain and gas pressure are the same in these spectra. Note the consistent parent ion dominance—indicative of predominant above threshold ionization-dissociation (ID)—particularly at 750 nm where there is less relative fragmentation compared to 375 nm. At both wavelengths daughter ions are seen to increase with increasing beam intensity. Doubly charged benzaldehyde is apparent as a strong peak at 750 nm.

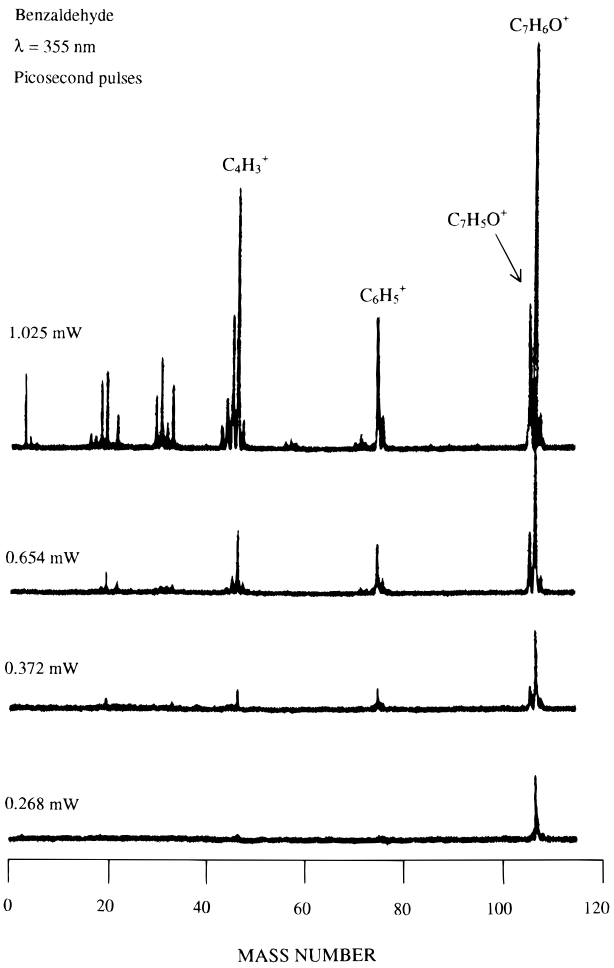

Figure 4. The 25 ps MPID mass spectrum of benzaldehyde at 355 nm at low to medium laser average power. Reproduced by kind permission of the authors of ref 1 and the American Chemical Society.

Figure 5 shows the ion yield as a function of laser intensity for 90 fs pulses for the main fragment mass peaks. In a multiphoton description of the process the appearance of the parent molecular ion implies absorption of at least 3 photons at 375 nm and 6 photons at 750 nm over the intensity range studied. From the gradients, a dependence of 2 for 375 nm and 3 for 750 nm were measured. This is consistent with a 3 (375 nm) and 6 (750 nm) multiphoton absorption process approaching saturation, which is expected at such high laser intensities.[29] The gradient of the benzaldehyde doubly charged ion is much greater than the other ions, which is also true for the H and C ions at 750 nm.

The mass spectra indicating the predominant initial appearance of parent molecular ions even at the lowest laser intensities suggest a common parent precursor in an above-threshold dissociation mechanism. Furthermore the consistent dominance of benzaldehyde parent ions over its moieties as the laser flux increases also supports an ID route. This parent supremacy was true for all pulse lengths used. In addition it can be seen that the mass fragments have the same slope as the parent ion at both wavelengths (apart from the doubly charged benzaldehyde ion and C and H at 750 nm), again suggesting a common parent precursor in an ID model.[8] If the DI route were dominant, then the gradient of the fragment moieties, whose appearance potentials are normally different from those of the parent, would not necessarily follow that of the parent as was evident from Figure 4. The principal DI route is C_6H_6 + CO as indicated in the Introduction. When these neutral molecules are irradiated individually as ground-state gases at high intensities, by far the predominant peaks in the mass spectra are the parent ions at mass 78 and 28, respectively.[28] In the present work these peaks are very small, which suggests that these neutral fragments are largely missing and thus the DI dissociative pathway is a minor one.

In the region of 10^{14} W cm^{-2}, saturation[29] of the parent ion signal is approached. This has been described as maximum sensitivity FLMS[30] and relates to unity ionization probability, which physically corresponds to all molecules within the sensitive volume being ionized, this volume being intimately related to the laser spot dimensions at the local region of ionization. Experimentally this is a reduction in the rate of change of ion yield as the laser intensity increases and can be seen as a characteristic bend at the uppermost curve locality. Any increase after this is mainly due to an expansion in the focal volume of the laser beam. This effect is more visible with 750 nm where slightly higher intensities were achievable.

Figure 6 shows the total ion yield (summing all peaks in the mass spectra) as a function of laser intensity at 750 and 375 nm and 90 fs. Saturation is apparent from the experimental yield curves and is also expected from the general considerations of multiphoton ionization cross sections[29] at laser intensities in excess of 10^{13} W cm^{-2}. In benzaldehyde, at 750 nm the

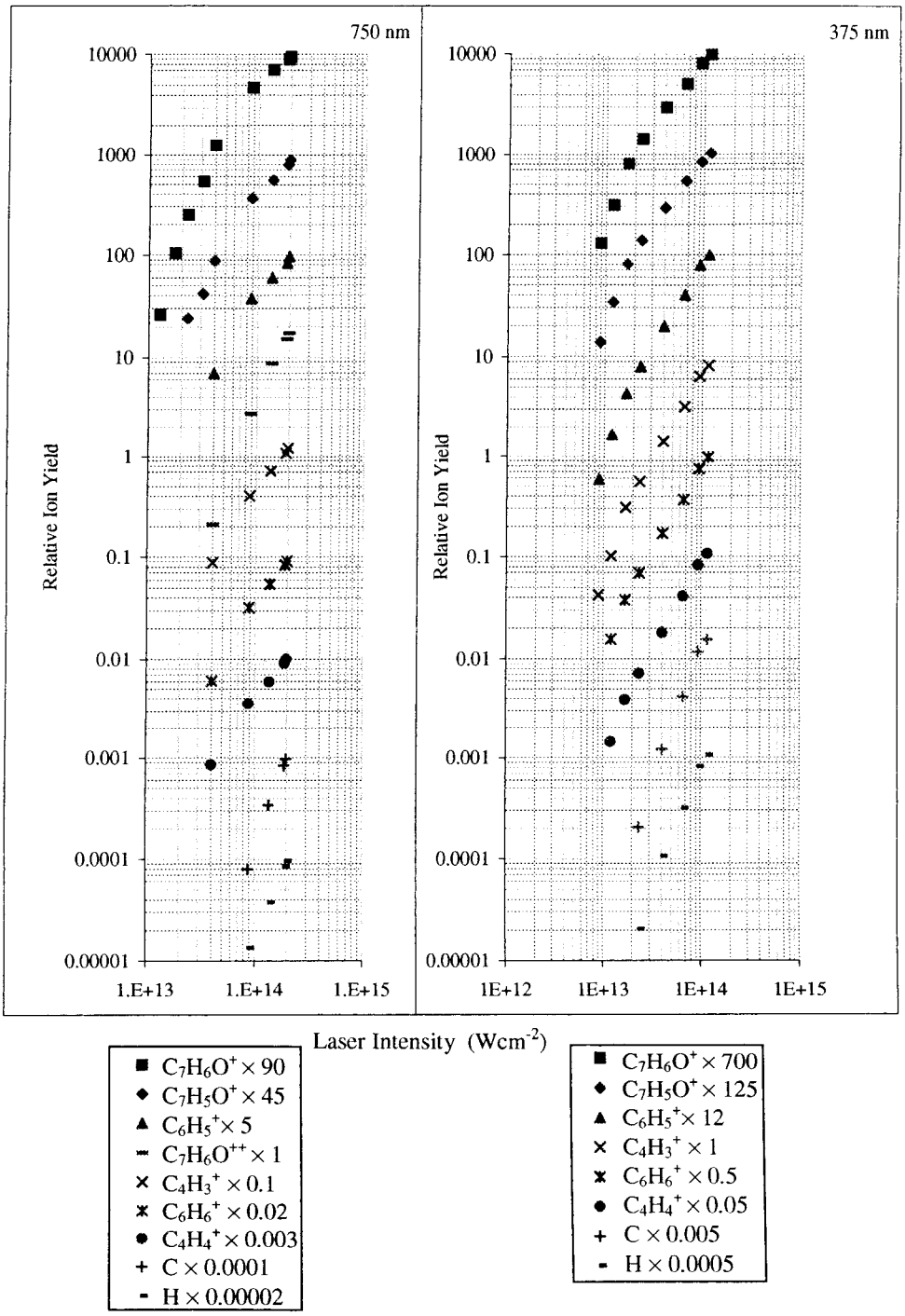

Figure 5. Relative ion yield as a function of laser intensity at 90 fs pulse widths for the main mass fragments. Vertical multiplication factors are indicated that serve to separate the ion plots. The ions are multiplied by these factors prior to drawing the graphs. Note how the general consistency of the gradients is suggestive of a common parent precursor in an ID model. The gradient of the doubly charged benzaldehyde ion as well as those for the H and C at 750 nm are much steeper. Also notice the approach to saturation of the parent ion signal for intensities in the region of 10^{14} W cm^{-2} at the uppermost section of the curve.

multiphoton transition proceeds with the absorption of 6 photons to reach the parent ion, while 375 nm ionization requires 3 photons. The predicted yields for the cross sections are shown in Figure 6 as a solid curve, and the agreement with the data is excellent. In calculating the theoretical curves, the effects due to the beam spot size, time profile of the laser pulse and the finite acceptance volume of the time-of-flight mass spectrometer have been taken into account. The cross sections for the six-photon (nonresonant) absorption for 750 nm and the three-photon absorption for 375 nm were treated as variable parameters in the fitting and were found to be $1.38e^{-180}$ cm^{14} s^5 and $1.5e^{-82}$ cm^6 s^2, respectively. Both sets of theoretical curves were normalized by the same factor for this comparison. The fitted cross sections are to be compared with the generalized cross sections of $3.2e^{-176}$ cm^{14} s^5 and $6.74e^{-81}$ cm^6 s^2 given by Ammosov et al.[31] for hydrogen atoms. The generalized cross section would produce saturation at much lower values of the laser intensity, particularly for 750 nm, and are not compatible with the experimental observations.

A series of experiments was carried out at different pulse widths in a manner described in the Experimental Section. These pulse widths have been shown to have similar bandwidths. For

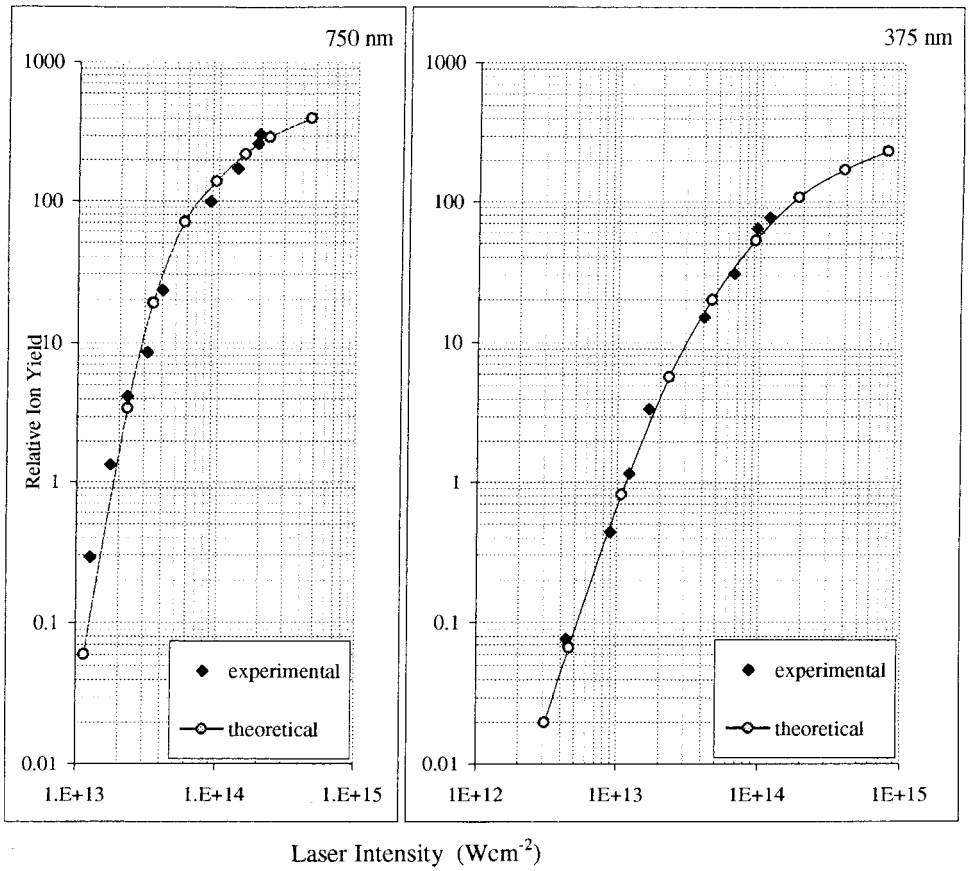

Figure 6. Total relative ion yield summed over all ions produced as a function of laser intensity for 90 fs at 750 and 375 nm. Both graphs are normalized consistently. In calculating the theoretical curves (solid curves), the effects due to the beam spot size, time profile of the laser pulse, and the finite acceptance volume of the time-of-flight mass spectrometer have been taken into account. The cross sections for the six-photon (nonresonant) absorption for 750 nm and the three-photon absorption for 375 nm were treated as variable parameters in the fitting and were found to be $1.38e^{-180}$ cm^{14} s^5 and $1.5e^{-82}$ cm^6 s^2, respectively. The agreement between theory and experiment is excellent.

the 750 nm wavelength, the pulse widths varied from 90 fs to 2.7 ps and for 375 nm from 90 fs to 1.3 ps. In Figure 7, four mass spectra showing the parent and the hydrogen loss peaks for different pulse widths at both wavelengths are shown. The ratios of parent to hydrogen loss for all the different pulse widths and the two wavelengths are shown in Figure 8. It is clear that the relative parent intensity grows as the pulse width decreases, an effect that is more significant at 750 nm. It must be emphasized that the ratios of parent to hydrogen loss at all pulse widths are only weakly dependent on the laser intensity, and the error bars in Figure 7 are a measure of this dependence. The data in Figures 7 and 8 suggest a hydrogen loss pathway with a dissociation time of about 1 ps.

Several authors have argued that when the laser intensity reaches 10^{14-15} W cm^{-2}, it is possible that field ionization (tunneling)[10,32-35] can provide a more complete description of the ionization mechanism than multiphoton theories. This is perhaps intuitive when one considers that associated electric fields at these high intensities match or even surpass molecular Coulombic fields felt by valence electrons, whose orbital periods are comparable to the laser pulse duration. The electric field of a high-intensity laser can cause severe modifications to the molecular potential energy surface resulting in the possibility of the valence electron(s) tunneling through the barrier formed by the molecular potential and the instantaneous electric field of the laser. For tunneling to take place in the ac field of the laser, the barrier must remain static for long enough to allow the electron to cross the barrier.

The Keldysh parameter[36] defined by

$$\gamma = (E_i/1.87 \times 10^{-13} I\lambda^2)^{1/2}$$

where E_i is the zero-field ionization potential expressed in eV, I is the laser intensity in W cm^{-2}, and λ is the laser wavelength in μm, has given a semiquantitative indication of the tunnel ionization mechanism.

Values of $\gamma < 0.5$ have been postulated as a pragmatic threshold for tunneling.[37] In the present experiment all values for γ are greater than unity. A number of authors have indicated that saturation in multiphoton ionization is expected to occur for intensities of the order of 10^{14} W cm^{-2}, which are lower than the intensities needed for tunneling to become important. The ionization is not purely multiphoton in the sense that tunneling has a small contribution to the total ionization rate.[29,38] The relative importance of multiphoton and tunneling ionization for high-intensity lasers needs to be examined in greater detail, particularly for larger molecules. In the view of the authors of the present paper, the multiphoton process is the principal mechanism for ionization/dissociation of molecules for laser intensities up to $\sim 10^{14}$ W cm^{-2}.

Conclusions

The mass spectra at 750 and 375 nm have been recorded at different pulse widths between 90 fs and 2.7 ps and for a range of laser intensities up to 1.2×10^{14} W cm^{-2}. The principle **points** that can be **concluded** from these data are as follows:

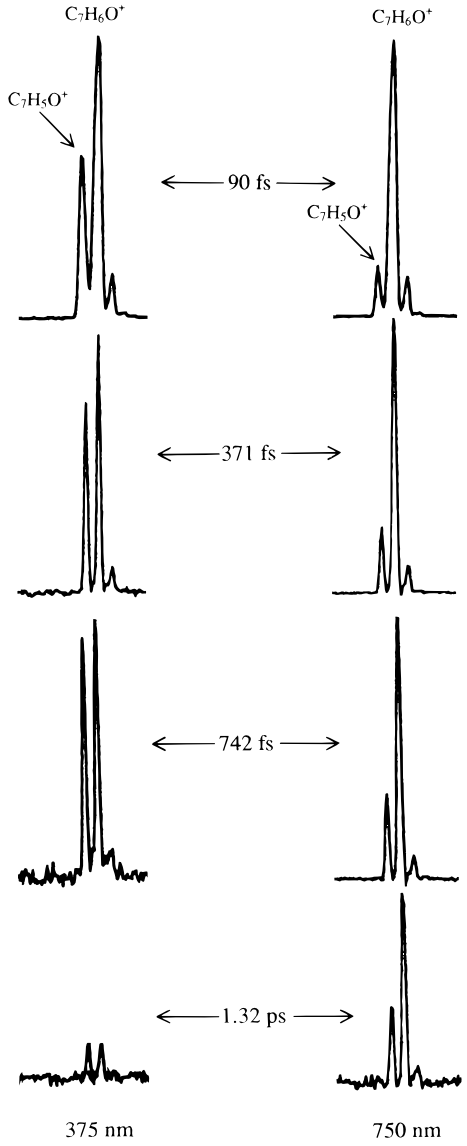

Figure 7. Mass spectra of the parent and hydrogen loss ion peaks for different pulse widths at 375 and 750 nm. For shorter pulse widths the dominance of the parent ion over its daughter increases. Evidence is also seen of protonation of the benzaldehyde ion.

(1) For the two wavelengths, the parent peak height dominates at all intensities and pulse widths.

(2) The parent peak alone is visible at the lowest intensities at all pulse widths and for both wavelengths. This soft ionization procedure is particularly important for analytical purposes especially with multicomponent samples. If one wishes high ionization efficiency with a predominant parent peak, then a high laser intensity at longer wavelengths is preferred.

(3) 375 nm gives more fragmentation by a factor of about 4 over that at 750 nm. This is difficult to explain unambiguously but is a characteristic of molecular dissociation at high intensities for a number of other molecules, e.g., NO_2, CO_2, CS_2, benzene, toluene, naphthalene, and 1,3-butadiene.[39] On the other hand, for the nitro aromatics the fragmentation becomes greater at 750 nm.[2,7] One of the obvious differences between the spectra in Figure 3 at 750 and 375 nm apart from the marked increase of fragmentation is the large doubly ionized benzaldehyde peak at 750 nm which is completely missing in the spectrum at 375 nm. The doubly ionized parent peak is also a prominent feature of a number of other molecules: CO_2, CS_2, CH_3I, benzene,

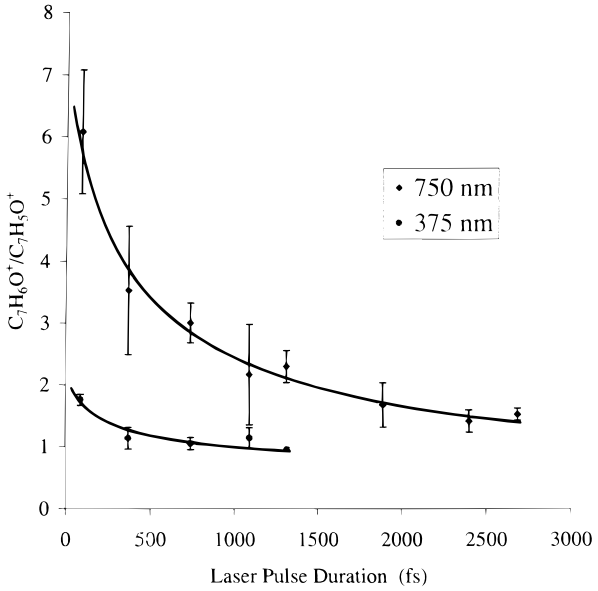

Figure 8. Ratio of the benzaldehyde ion to its hydrogen loss daughter as a function of pulse width at 750 and 375 nm. The relative parent intensity grows as the pulse width decreases, an effect that is more pronounced at the longer wavelength where a greater relative number of ions are produced. At any given pulse width, $C_7H_6O^+/C_7H_5O^+$ shows only a weak laser intensity dependence. The points represent the mean ratio value, while the error bars indicate this weak intensity dependence as the standard deviation.

toluene, naphthalene, and 1,3-butadiene[39] at laser intensities of about 10^{14} W cm^{-2}. The observation of doubly ionized medium mass hydrocarbons points to considerable structural stability of these ions. How the charges reside on such a molecule without blowing apart is an interesting question.

(4) The relative ion yields for the parent and principal fragment ions have been measured as a function of the laser intensity at the two wavelengths. The gradients are similar for all the species suggesting a common parent precursor which is characteristic of ID. Apart from doubly ionized benzaldehyde, C and H, the measured slopes of 3 and 2 for the principal fragments at 750 and 375 nm respectively indicate that the process is approaching saturation in a multiphoton model. The total ion yields also show signs of saturation. The data can be fitted closely using a rate equation model and off-resonant multiphoton cross sections.

(5) The ratio of the ions C_7H_6O/C_7H_5O is almost independent of laser intensity for a given pulse width. However it varies considerably as the laser pulse width changes, increasing as the pulse width decreases. This is characteristic of an H loss dissociative time on the order of a picosecond, although it is unlikely to be the only mechanism of producing the H loss fragment. Using 25 ps pulses, Yang et al. are also in agreement with this short dissociation time, having suggested that there was an immediate fragmentation of the parent ion into $C_7H_5O^+$. This behavior also occurs with recent results[30] for NO_2^+/NO^+ under similar experimental conditions

Acknowledgment. D.J.S., K.W.D.L., H.S.K., R.P.S., T.McC., W.X.P., and C.K. would like to express thanks to Rutherford Appleton Lab (R.A.L.) for excellent facilities and assistance. D.J.S., H.S.K., and W.X.P. also acknowledge the EPSRC, the Turkish Government, and the University of Glasgow respectively for financial support.

References and Notes

(1) Yang, J. J.; Gobeli, D. A.; El-Sayed, M. A. *J. Phys. Chem.* **1985**, *89*, 3426.
(2) Kilic, H. S.; Ledingham, K. W. D.; Kosmidis, C.; McCanny, T.; Singhal, R. P.; Wang, S. L.; Smith, D. J.; Langley, A. J.; Shaikh, W. *J. Phys. Chem. A* **1997**, *101*, 817.
(3) Gedanken, A.; Robin, M. B.; Keubler, N. A. *J. Phys. Chem.* **1982**, *86*, 4096.
(4) Ledingham, K. W. D.; Kosmidis, C.; Georgiou, S.; Couris, S.; Singhal, R. P. *Chem. Phys. Lett.* **1995**, *247*, 555.
(5) Singhal, R. P.; Kilic, H. S.; Ledingham, K. W. D.; Kosmidis, C.; McCanny, T.; Langley, A. J.; Shaikh, W. *Chem. Phys. Lett.* **1996**, *81*, 253.
(6) Ledingham, K. W. D.; Kilic, H. S.; Kosmidis, C.; Deas, R. M.; Marshall, A.; McCanny, T.; Singhal, R. P.; Langley, A. J.; Shaikh, W. *Rapid Commun. Mass Spectrom.* **1995**, *9*, 1522.
(7) Kosmidis, C.; Ledingham, K. W. D.; Kilic, H. S.; McCanny, T.; Singhal, R. P.; Langley, A. J.; Shaikh, W. *J. Phys. Chem. A* **1997**, *101*, 2264.
(8) Ledingham, K. W. D.; Singhal, R. P. *Int. J. Mass. Spectrom. Ion Processes* **1997**, *163*,149.
(9) Vijayalakshmi, K.; Safran, C. P.; Ravindra Kumar, G.; Mathur, D. *Chem. Phys. Lett.* **1997**, *270*, 37.
(10) Codling, K.; Frasinski, L. J. *J. Phys. B: At. Mol. Opt. Phys.* **1993**, *26*, 783.
(11) Weinkauf, R.; Aicher, P.; Wesley, G.; Grotemeyer, J.; Schlag, E. W. *J. Phys. Chem.* **1994**, *98*, 8381.
(12) He, C.; Basler, J. N.; Becker, C. H. *Nature* **1997**, *385*, 797.
(13) Brummel, C. L.; Willey, K. F.; Vickerman, J. C.; Winograd, N. *Int. J. Mass Spectrom. Ion Processes* **1995**, *143*, 257.
(14) Grun, C.; Weickhardt, J.; Grotemeyer, J. *European Mas Spectrom.* **1996**, *2*,197.
(15) Schutze, M.; Trappe, C.; Tabellion, M.; Lupke, G.; Kurz, H. *Surf. Interface Anal.* **1996**, *24*, 399.
(16) Silva, C. R.; Reilly, J. P. *J. Phys Chem.* **1996**, *100*, 17111.
(17) Long, S. R.; Meek, J. T.; Harrington, P. J.; Reilly, J. P. *J. Chem. Phys.* **1983**, *78*, 3341.
(18) Yang, J. J.; Gobeli, D. A.; Pandolfi, R. S.; El-Sayed, M. A. *J. Phys. Chem.* **1983**, *87*, 2255.
(19) Hirata, Y.; Lim. E. C. *J. Chem. Phys.* **1980**, *72*, 5505.
(20) Berger, M.; Goldblatt, I. L.; Steel, C. *J. Am. Chem. Soc.* **1973**, *95*, 1717.
(21) Antonov, V. S.; Letokhov, V. S. *Appl. Phys.* **1981**, *24*, 89.
(22) DeCorpo, J. J.; Hudgens, J. W.; Lin, M. C.; Saalfield, F. E.; Seaver, M. E.; Wyatt, J. R. *Adv. Mass. Spectrom.* **1980**, *8A*, 133.
(23) Seaver, M. E.; Hudgens, J. W.; DeCorpo, J. J. *Int. J. Mass. Spectrom. Ion. Phys.* **1980**, *34*, 159.
(24) Antonov, V. S.; Letokhov, V. S.; Shibanov, A. N. *Appl. Phys.* **1980**, *22*, 293.
(25) Hutchinson, M. H. R. *Contemp. Phys.* **1989**, *30*, 355.
(26) Langley, A. J.; Noad, W. J.; Ross, I. N.; Shaikh, W. *Appl. Opt.* **1994**, *33*, 3875.
(27) Langley, A. J.; Noad, W. J.; Ross, I. N.; Shaikh, W. *Central Laser Facility Annual Report* **1993** *RAL-93-031*, 224.
(28) Ledingham, K. W. D.; Kilic, H. S.; McCanny, T.; Peng, W. X.; Smith, D. J.; Singhal, R. P.; Kosmidis, C.; Langley, A. J.; Taday, P. F., to be published
(29) He, C.; Becker, C. H. *Phys. Rev. A* **1997**, *55*, 1300.
(30) Singhal, R. P.; Kilic, H. S.; Ledingham, K. W. D.; McCanny, T.; Peng, W. X.; Smith, D. J.; Kosmidis, C.; Langley, A. J.; Taday, P. F., to be published.
(31) Ammosov, M. V.; Delone, N. B.; Ivanov, M. Yu.; Bondar, I. I.; Masalov, A. V. *Adv. At. Opt. Phys.* **1992**, *29*, 33.
(32) Chin, S. L.; Liang, Y.; Decker, J. E.; Ilkov, F. A.; Ammosov, M. V. *J. Phys. B: At. Mol. Opt. Phys.* **1992**, *25*, L249.
(33) Augst, S.; Meyerhofer, D. D.; Strickland, D.; Chin, S. L. *J. Opt. Soc. Am. B* **1991**, *8*, 4.
(34) Gibson, G.; Luk, T. S.; Rhodes, C. K. *Phys. Rev. A* **1990**, *41*, 5049.
(35) Walsh, T. D. G.; Decker, J. E.; Chin, S. L. *J. Phys. B: At. Mol. Opt. Phys.* **1993**, *26*, L85.
(36) Keldysh, L. V. *Sov. Phys. JETP* **1965**, *20*, 1307.
(37) Ilkov, F. A.; Decker, J. E.; Chin, S. L. *J. Phys. B* **1992**, *25*, 4005.
(38) Talebpour, A.; Larochelle, S.; Chin, S. L. *J. Phys. B: At. Mol. Opt. Phys.* **1997**, *30*, L245.
(39) Smith, D. J.; Ledingham, K. W. D.; Kilic, H. S.; McCanny, T.; Peng, W. X.; Singhal R. P.; Langley A. J.; Taday P. F.; Kosmidis, C., to be published.